

A study of the large-scale distribution of galaxies in the South Galactic Pole region – II. Further evidence for a preferential clustering scale?

S. Ettori,^{1,2} L. Guzzo¹ and M. Tarenghi³

¹*Osservatorio Astronomico di Brera, Via Bianchi 46, I-22055 Merate (CO), Italy*

²*Institute of Astronomy, University of Cambridge, Madingley Road, Cambridge CB3 0HA*

³*European Southern Observatory, Karl Schwarzschild Strasse 2, D-85748 Garching, Germany*

Accepted 1996 September 30. Received 1996 August 28

ABSTRACT

We analyse a set of new pencil-beam galaxy redshift data in three small regions around the South Galactic Pole area. We investigate whether we can find any evidence of the quasi-periodic peaks discovered by Broadhurst et al. in the distribution of galaxies along the North Galactic Pole–South Galactic Pole directions. We use both a power spectrum analysis and a cross-correlation with a sliding comb-like window (the comb-template technique). Despite the data being less deep ($\sim 600 h^{-1}$ Mpc) and certainly not optimal for such an investigation, there is evidence of the same preferential $\sim 130 h^{-1}$ Mpc scale in two fields displaced respectively 15° and 30° west of the Broadhurst et al. original probe. Taken alone, however, this scale would not be statistically distinguishable from a noise fluctuation. Nevertheless, the statistical significance rises to ~ 99 per cent when one refers to the *conditional* probability of finding a peak around the *same* scale measured by Broadhurst et al.

Key words: surveys – galaxies: distances and redshifts – galaxies: general – large-scale structure of Universe.

1 INTRODUCTION

Deep ‘pencil-beam’ surveys (angular size $\sim 1^\circ$, depth $\sim 10^3 h^{-1}$ Mpc) (Koo & Kron 1987; Broadhurst, Ellis & Shanks 1988) have produced important results about the large-scale structure of the Universe. They are complementary to the wide-angle surveys (100° or larger, but with depth of only $100\text{--}200 h^{-1}$ Mpc; e.g. Giovanelli & Haynes 1991, Strauss & Willick 1995 and Guzzo 1996). These narrow shots through deep space provide a confirmation of strong inhomogeneities in the galaxy distribution up to scales of $50\text{--}100 h^{-1}$ Mpc.

One of the most exciting results obtained from pencil-beam surveys has been the detection, along the North Galactic Pole–South Galactic Pole (NGP–SGP) axis, of a typical scale in the distribution of galaxy concentrations, corresponding to a characteristic separation of $128 h^{-1}$ Mpc (Broadhurst et al. 1990, hereafter BEKS). This result is consistently confirmed by extensions of the original data set (Broadhurst et al. 1995), by independent galaxy surveys in nearby areas, as the ESO Slice Project (ESP, Vettolani et al. 1995), and by the large-scale distribution of clusters of galaxies (Bahcall 1991; Guzzo et al. 1992; Tully et al. 1992).

This latter evidence shows how at least the first maxima do coincide with large-scale 3D structures, and are not artefacts produced by an aliasing effect as claimed by Kaiser & Peacock (1991). However, what the periodicity precisely means in terms of large-scale structure is still controversial (e.g. Dekel et al. 1992). A similar effect would be expected in only 15 per cent of all directions in phenomenological Voronoi models (e.g. van de Weygaert 1991).

A clearer picture will probably arise only from new pencil-beam observations in different directions (see Broadhurst et al. 1995), together with a detailed knowledge of the 3D power spectrum of density fluctuations on $\lambda > 100 h^{-1}$ Mpc. With this paper, we try to add a small contribution in this direction, by analysing some new redshift data in the SGP area. Throughout the paper, we use $H_0 = 100 h \text{ km s}^{-1} \text{ Mpc}^{-1}$ and $\Omega_0 = 1$.

2 DATA GLOBAL PROPERTIES

2.1 The data

We use the redshift data discussed in Ettori, Guzzo & Tarenghi (1995, Paper 1 hereafter), where full details about

the observing strategy and the data reduction procedures can be found. These redshifts were collected using the 33-arcmin field ESO fibre spectrograph OPTOPUS in three regions around the SGP, named PW, PL and FD, for each of which we summarize here the salient aspects. The completeness of each field at different magnitude limits is given in Table 1.

Field PW contains 53 redshifts, in the area comprised between $22^{\text{h}}35^{\text{m}} < \alpha < 22^{\text{h}}40^{\text{m}}$ and $-29^{\circ} < \delta < -27^{\circ}45'$, limited to $b_j \leq 19.5$.

Field PL contains 415 redshifts, limited to $b_j \leq 19.62$. It extends between $23^{\text{h}}39^{\text{m}} < \alpha < 23^{\text{h}}52^{\text{m}}$ and $-29^{\circ} < \delta < -27^{\circ}45'$, centred on the rich cluster Klemola 44 (Abell 4038). With a mean velocity $\langle cz \rangle \simeq 8800 \text{ km s}^{-1}$, the cluster overdensity dominates the redshift distribution in this beam, contributing ~ 150 galaxies (34 per cent of the total). In fact, the main aim of the original survey was to study in detail the kinematics and structure of K44 and its surroundings (Ettori et al. 1996, in preparation). Despite this bias towards a specific redshift peak, the faint magnitude limit of the survey provides a large number of foreground and background redshifts. To exclude the cluster effect, we also ana-

lyse separately the subsample of 288 galaxies lying at $cz > 11\,500 \text{ km s}^{-1}$, that we call PL-K44.

Field FD is composed by five non-contiguous OPTOPUS fields (see Paper 1), located between $2^{\text{h}}01^{\text{m}} < \alpha < 2^{\text{h}}16^{\text{m}}$ and $-30^{\circ}10' < \delta < -28^{\circ}15'$, $\sim 30^{\circ}$ east of the BEKS probe, containing 54 galaxies limited to $b_j \leq 19.5$.

2.2 The selection function

The comoving distance for all the galaxies in the sample is evaluated as

$$d_c = \frac{c}{H_0 q_0^2 (1+z)} [q_0 z + (q_0 - 1)(-1 + \sqrt{2q_0 z + 1})], \quad (1)$$

with $q_0 = 0.5$. The results discussed in the following do not change significantly using $q_0 = 0.1$. The selection function can be then calculated by integrating the Schechter luminosity function,

$$\Phi(L) d(L) = \Phi^* \left(\frac{L}{L^*} \right)^\alpha e^{-L/L^*} d\left(\frac{L}{L^*} \right), \quad (2)$$

to the magnitude limit of each field. However, in order to take properly into account the magnitude-dependent incompleteness evident from Table 1, we estimate the actual selection function separately for four apparent-magnitude bins. In other words, we normalize to a different ϕ^* within each bin, and then calculate the global selection function as

$$\phi(d_c) = \sum_1^4 \int_{M_i(b_j, d_c)}^{M_{i+1}(b_j, d_c)} \Phi(\Phi^*_i, M) dM. \quad (3)$$

For the shape parameters of the luminosity function, we adopt the very recent estimate from the ESP survey (Zucca et al. 1996), that finds $M^* = -19.57$ and $\alpha = -1.22$. This estimate of the luminosity function is optimal for our data, having been performed on the same parent photometric catalogue (the Edinburgh/Durham Southern Galaxy Catalogue, EDSCG) and to a very similar magnitude limit. The selection function also takes into account the K -correction, calculated following Shanks et al. (1984), assuming an early-type/late-type ratio of 0.3/0.7. This hypothesis is necessary, the morphological type being unknown for most of our galaxies.

Fig. 1 shows the resulting $\phi(d_c)$ for the three regions plotted on top of the observed distribution in bins of $30 h^{-1} \text{ Mpc}$ (shaded histogram). In the same figures we show also the result of normalizing the data to the total number of galaxies expected from the parent photometric catalogue, again considering separately the completeness for each b_j -magnitude bin (open histogram).

2.3 Data sparseness

Before starting to look for possible periodic patterns in our data, we asked ourselves whether the data at least good enough to answer the zero-order question: 'is the data distribution significantly different from a random distribution observed with the same selection function?' One way to

Table 1. Completeness in the three fields at different magnitude limits. n_{stars} is the number of objects found to be misclassified stars in the EDSCG and therefore excluded a posteriori from the sample (see Paper 1). n_z is the actual number of *galaxy* redshifts available. Note that the completeness is estimated in a conservative manner, i.e. assuming that the remaining unobserved objects in the target catalogue are all galaxies. If one applied the stellar contamination percentages to the entire parent catalogues, the observed completeness would improve by a few per cent, essentially in the fainter magnitude bins.

	n_{EDSCG}	n_{stars}	n_z	Compl.(%)
$b_j < 18.0$	187	4	149	81.4
$18.0 \leq b_j < 18.5$	90	5	54	63.5
$18.5 \leq b_j < 19.0$	173	21	70	46.1
$19.0 \leq b_j \leq 19.62$	359	29	142	43.0
<i>tot</i>	809	59	415	55.3
field PW				
	n_{EDSCG}	n_{stars}	n_z	Compl.(%)
$b_j < 18.0$	26	6	14	70.0
$18.0 \leq b_j < 18.5$	21	4	10	58.8
$18.5 \leq b_j < 19.0$	39	7	18	56.3
$19.0 \leq b_j \leq 19.5$	25	6	11	57.9
<i>tot</i>	111	23	53	60.2
field FD				
	n_{EDSCG}	n_{stars}	n_z	Compl.(%)
$b_j < 18.0$	13	0	10	76.9
$18.0 \leq b_j < 18.5$	13	1	10	83.3
$18.5 \leq b_j < 19.0$	47	5	15	35.7
$19.0 \leq b_j \leq 19.5$	85	10	19	25.3
<i>tot</i>	158	16	54	38.0

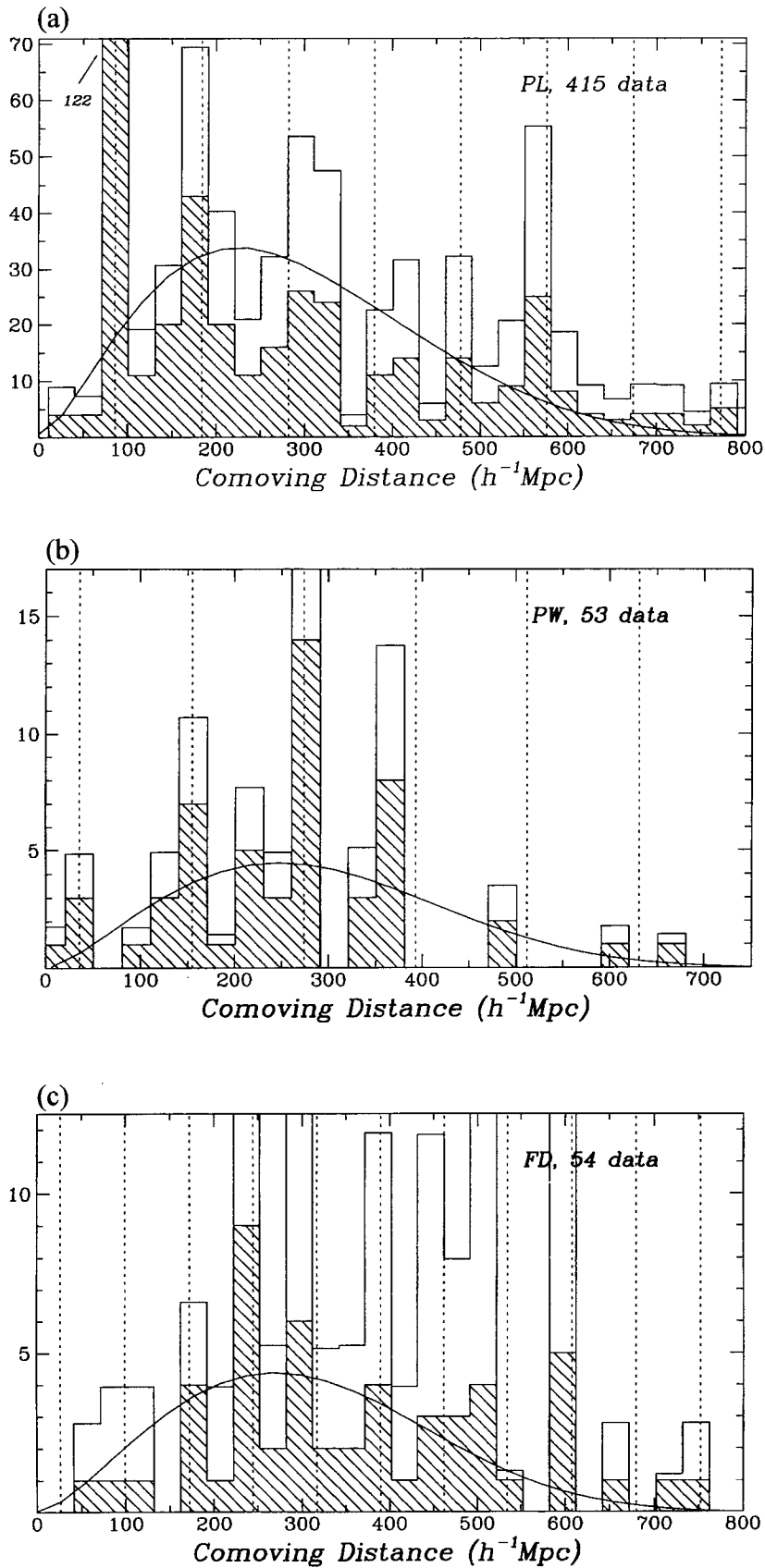


Figure 1. (a) Redshift distribution in $30 h^{-1} \text{Mpc}$ bins in the PL field. The shaded histogram is the observed distribution, while the open histogram shows the result of normalizing each apparent magnitude bin for the completeness, as shown in Table 1 and discussed in the text. The solid curve is the selection function calculated using equation 3. Vertical dashed lines indicate the best periodicity as obtained in Section 3. (b) The same, for field PW. (c) The same, for field FD.

quantify this difference is to calculate the so-called double-root residuals (DRRs). This method compares an observed distribution function with a model by estimating properly weighted residuals (Gebhardt & Beers 1991). Residuals are normally calculated giving equal weight to both low-populated bins, generally belonging to the tails of the distribution, as to central bins containing many more data points. Since the residuals depend strictly on \sqrt{N}/N fluctuations, they are not a correct diagnostic of the agreement between the data and the model all over the range covered by the distribution. The DRR method introduces a square-root transformation, which appropriately weights the residuals of the different bins, showing *where* there is a significant deviation of the data from the model. If B_i is the data value of bin i and M_i is the corresponding model value, the DRRs are defined as:

$$\text{DRR}_i = \sqrt{2 + 4B_i} - \sqrt{1 + 4M_i} \quad \text{if } B_i \geq 1, \quad (4)$$

$$\text{DRR}_i = 1 - \sqrt{1 + 4M_i} \quad \text{if } B_i = 0.$$

The local deviations of the DRRs for the given model (assumed to describe sufficiently well the global trend of the data), give directly a confidence level in terms of standard deviations. To reject the null hypothesis at the 95 per cent confidence level, for example, we will require bins with $|\text{DRR}| > 2$.

Fig. 2 shows the DRRs for our data, when compared with the selection function. For PW and FD the null hypothesis can be rejected at the 95 per cent confidence level only for

a few bins. This already tells us not to expect to obtain much significant statistical information from these two data sets. On the contrary, PL shows rather significant fluctuations, with peaks in correspondence to K44 and to 170 and $570 h^{-1}$ Mpc and troughs around 250, 350 and $450 h^{-1}$ Mpc.

3 PERIODICITY ANALYSIS

Having established that the data show at least some deviations from an uniform distribution, we address now the question of the presence within the three regions of any significant periodic pattern similar to that originally found by BEKS. To this end, we apply two statistics, the classical power spectrum analysis, and the so-called comb-template test.

3.1 The power spectrum analysis

Considering a set of N data with comoving distance d_j , we define the *power spectrum* as the quantity

$$P_k = \frac{1}{N} \left| \sum_{j=1}^N e^{i2\pi k d_j} \right|^2. \quad (5)$$

This can be seen as the squared amplitude of a discrete Fourier transform of $N \delta_{\text{Dirac}}$ functions, each located at position d_j corresponding to the galaxy positions. Under the null hypothesis of a uniform galaxy distribution on scales

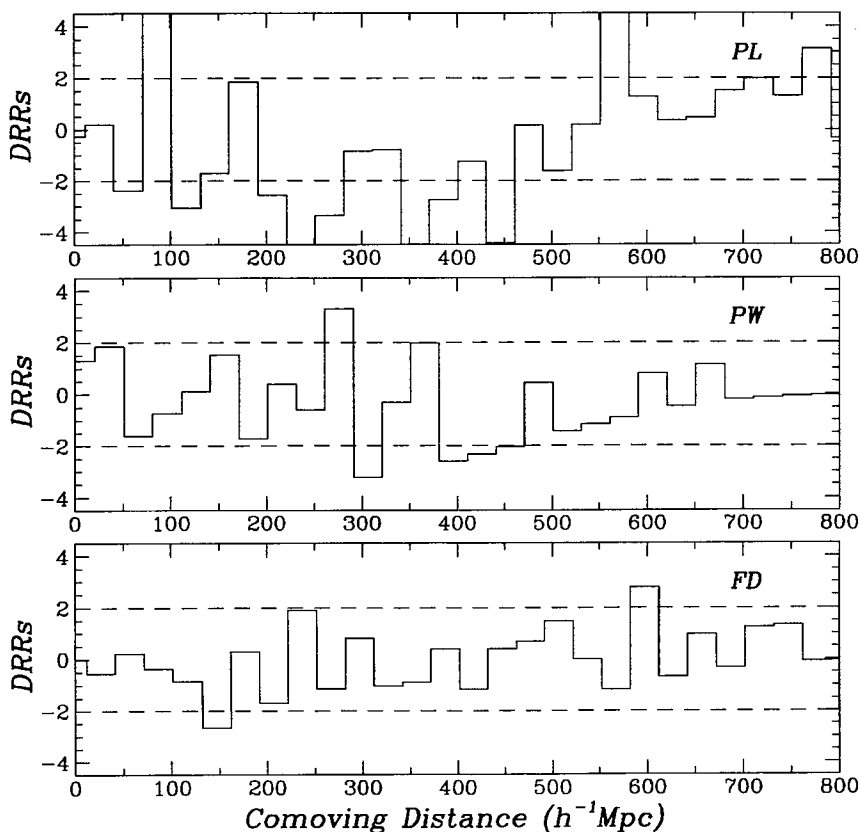


Figure 2. The results of the DRRs analysis, showing the significance of the fluctuations in the data with respect to the null hypothesis of a uniform distribution with the same selection function. The dashed lines at ± 2 indicate the 95 per cent significance level.

$> 30 h^{-1}$ Mpc (Szalay et al. 1991), the probability distribution of P_k is equal to a $\chi^2(2)/2$ distribution, i.e. an exponential (since the real and imaginary parts of the Fourier coefficients are Gaussian distributed and statistically independent; cf. Burbidge & O'Dell 1972; see Amendola 1994 for the non-Gaussian case). The expectation value of this distribution is unity. To explore the significance level of any power P_k present in the spectrum, let us consider the new variable $z_k = P_k / \langle P_k \rangle$, where $\langle P_k \rangle$ is the mean power in the spectrum. The observed distribution of z_k will have a mean which is 1 by definition. We can then evaluate the significance of any observed power by comparing it with the null hypothesis, still described by an exponential.

It can be shown (cf. Burbidge & O'Dell 1972, Szalay et al. 1991) that for K -independent test wavenumbers the significance level of any peak z_k^h in the power spectrum is given by

$$p(z_k > z_k^h) = 1 - [1 - \exp(-z_k^h)]^K. \quad (6)$$

To establish the significance of a peak, we need therefore to estimate the two parameters $\langle P_k \rangle$ and K for each field. $\langle P_k \rangle$ is the mean power estimated on the K wavenumbers; K can be calculated as

$$K = \frac{k_{\max} - k_{\min}}{\Delta k}, \quad (7)$$

where k_{\max} and k_{\min} correspond respectively to the inverse of the minimum and maximum scale that we chose to analyse (see below). Δk is the spacing in wavenumber between two contiguous k 's, i.e. the smallest independent frequency and/or the largest comoving range, that for our case corresponds to $\Delta k = 1/d_{j,\max} - d_{j,\min} = 1/700$. For our data, we limit the range of investigation to scales between 30 and $400 h^{-1}$ Mpc, i.e. within a range where we can neglect the

effects of small-scale clustering ('red noise') and of the uncertainty on the selection function at large distances. These yield $k_{\max} = 0.0333$ and $k_{\min} = 0.0025 h \text{ Mpc}^{-1}$.

To produce a smoother picture of the power spectrum, we oversampled the number of wavenumbers, as shown in Fig. 3, i.e. calculating the power at 'dependent' wavenumbers separated by less than $\Delta k = 1/700$. It should be clear that this oversampling does not add any contribution to the significance level of an investigated power.

The final results are shown in Fig. 3 and listed in Table 2. None of the peaks observed in the different fields provides a statistically significant evidence for a preferred clustering scale. The probability that the highest peak is simply a random fluctuation of the noise is everywhere larger than 20 per cent. However, it is worth noticing how for PL-K44 and PW the value of the most probable period is interestingly close to the BEKS value of $128 h^{-1}$ Mpc.

3.2 The comb-template test

The comb-template test (CT hereafter), has been used by Duari, Das Gupta & Narlikar (1992) to look for periodicity in the distribution of QSOs. Its main advantage is to be able to identify, in a simple way, the starting point of a periodicity (i.e. its phase), providing also a relative probability value for the more significant period.

Table 2. Results of the power spectrum analysis. T_{peak} is the period corresponding to the highest peak detected. P_{peak} is the height of the peak. $\langle P_k \rangle$ is the mean noise level, and p is the probability that the peak is a random noise fluctuation.

	T_{peak} (h^{-1} Mpc)	P_{peak}	$\langle P_k \rangle$	p
PL	98.0	43.72	11.41	0.355
PL-K44	128.2	21.10	5.66	0.371
PW	119.0	11.28	2.64	0.225
FD	72.5	7.15	1.85	0.445

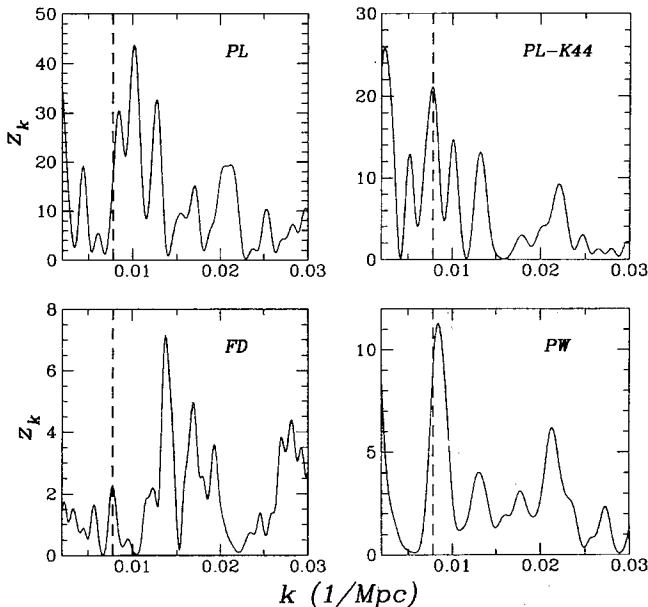


Figure 3. Power spectra for the four data sets analysed. The vertical dashed lines correspond to the $128 h^{-1}$ Mpc BEKS periodicity ($k \approx 0.0078 h \text{ Mpc}^{-1}$).

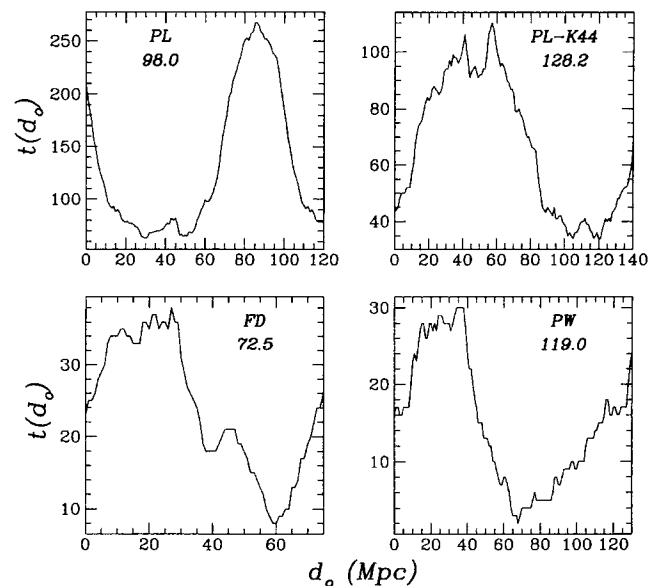


Figure 4. The distribution of the phases d_0 from the comb-template test. The period adopted (as obtained from the power spectrum), is reported for each data set.

Assuming that the objects are concentrated within peaks of width w , spaced with a period D , we slide a comb-like template with periodic ‘teeth’ across the galaxy redshift distribution and evaluate the function

$$c(d_i, d_0) = \begin{cases} 1 & \text{if } \left| d_i - \left[d_0 + D \operatorname{nint} \left(\frac{d_i - d_0}{D} \right) \right] \right| < w/2, \\ 0 & \text{otherwise,} \end{cases} \quad (8)$$

where d_0 is the starting point and $\operatorname{nint}(x)$ is the nearest integer to x .

For a discrete distribution of δ_{Dirac} functions, the test consists in evaluating the correlation function

$$t(d_0) = \sum_{i=1}^N c(d_i, d_0). \quad (9)$$

For an uniform galaxy distribution, it can be shown that $t(d_0)$ has the a mean value $\mu = Nw/D$ and standard deviation $\sigma_i = \sqrt{\mu(1-w/D)}$. The highest value of $t(d_0)$, t_{\max} , corresponds to the most probable starting point d_0 . In addition, given a test period the null hypothesis of a uniform distribution can be rejected at the $n\sigma$ confidence level if t_{\max} is larger than μ by the same amount. Fig. 4 shows the behaviour of $t(d_0)$ for our four samples, when the D parameter is fixed to the value obtained from the power spectrum analysis and the width w is set to 15 Mpc. We did not find any significant dependence of the results on variations of this latter parameter. Note that the d_0 is measured from the lower limit of the data set in comoving distances, which for the PL-K44 sample corresponds to the redshift cut at $cz = 11\,500 \text{ km s}^{-1}$.

A second interesting step is to compare the values of t_{\max} obtained for different periods, to find which period corresponds to the ‘least random’ distribution. The results of this

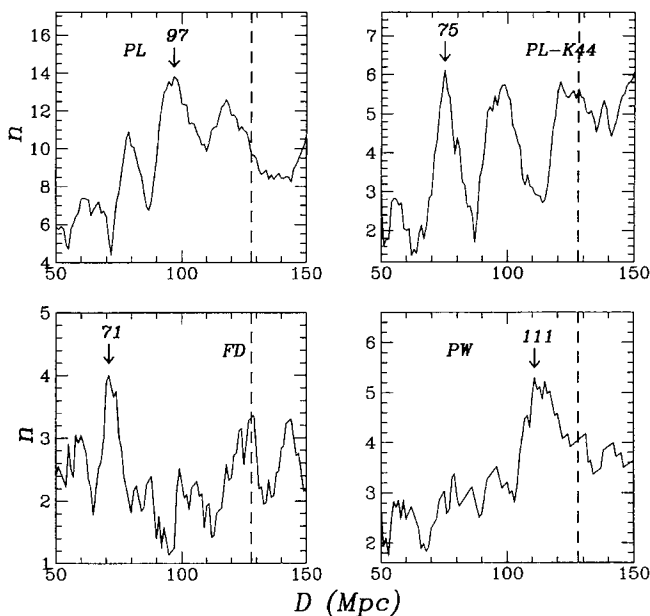


Figure 5. The distribution of the test periods from the comb-template test. n gives the number of σ deviations from a uniform distribution, for any given D . The arrows mark the highest peak, corresponding to the best period. The BEKS periodicity is given by the dashed lines.

test, performed on scale between 50 and 200 Mpc, are shown in Fig. 5. This analysis is conceptually different from the power spectrum, but, as can be seen in the figure, it provides a substantial confirmation of the results of the harmonic analysis. Only in one case (PL-K44), there is some evidence for a different specific scale at $D \sim 70$ Mpc, which, interestingly, has a similar counterpart also in field FD. We summarize the results of the CT test in Table 3.

4 DISCUSSION AND CONCLUSIONS

Let us discuss first the case of the field PL, where the situation is complicated by the dominating overdensity of the K44 cluster of galaxies. In fact, the power spectrum (Fig. 3, upper panels) shows a number of peaks, with no particular preference for the BEKS scale. The main ‘period’ which arises from both the power spectrum and the CT test (Fig. 5), clearly corresponds to the separation between the cluster and the second redshift peak, $\sim 98 h^{-1}$ Mpc. The critical effect of the cluster on the harmonic analysis is also evidenced by the value of the starting point provided by the CT test – i.e. the phase of the hypothetical ‘periodicity’ – which correspond exactly to the position of the cluster ($85\text{--}86 h^{-1}$ Mpc). It is interesting to note, however, that when the cluster is removed from the sample, a peak arises in P_k right at the BEKS scale, although it is just slightly more than a $\sim 1\sigma$ fluctuation and therefore not statistically significant.

The field PW is the only one with a dominant peak in the power spectrum, corresponding to a period $\sim 120 h^{-1}$ Mpc. Also in this case, however, its significance is low, owing to the sparseness of the data evidenced by the DRRs: the null hypothesis can be rejected only at the 77 per cent confidence level. The CT test shows the same tendency for a preferential scale around a similar value.

In the field FD there is some consistency for a preferred scale at $\sim 70 h^{-1}$ Mpc from both the P_k and CT analyses. However, the significance of this peak is even lower than for the other fields (with a 54 per cent confidence level). We mention it for two reasons: first, because the CT test shows a similar scale also for the field PL-K44; secondly, because a similar scale was detected by Mo et al. (1992) in their analysis of a number of different samples, and is close to a kind of second harmonic of the BEKS scale.

Table 3. Results of the comb-template test. d_0 is the most probable value for the phase (i.e. the starting point), of a periodic pattern having the period as yielded by the power spectrum. n_σ is the confidence level (in number of σ s), with which the null hypothesis of a uniform distribution can be rejected. D_{\max} is the most probable period obtained by the test when d_0 is left as a free parameter. $n_{\sigma-\max}$ is its confidence level, again in terms of standard deviations, as defined in the text.

	d_0 (h^{-1} Mpc)	n_σ	D_{\max} (h^{-1} Mpc)	$n_{\sigma-\max}$
PL	85	13.69	97	13.81
PL-K44	57	5.11	75	6.11
PW	36	4.54	111	5.29
FD	27	3.87	71	4.00

So far we have considered the simple absolute significance of the potential periods evidenced by our analysis. In other words, we have asked ourselves whether in our three sets of data there is any significant evidence for a regularity with a preferred scale in the galaxy one-dimensional distribution. The answer to this question is clearly negative: we have shown how our set of data is essentially not good enough on its own for this purpose.

However, there is a more specific question that we can ask, i.e. given the three independent data sets, is there any evidence for a peak in the power spectrum around the same value found by BEKS, and how significant is it? The answer to this second question is more interesting, as we have seen that in two directions, PL and PW, there is indeed a peak around that same scale. The significance level of this event will be now given by the conditional probability of the two events of (1) having a peak of that height anywhere in the explored range, and (2) finding it around $130 h^{-1}$ Mpc. In practice, this results is the product of the absolute probability estimated in Table 2, with the inverse of the number of frequencies explored, which is 22 in our case. This gives a probability of 1.4 per cent for PL and 1 per cent for PW (almost 99 per cent confidence level) that a scale of $120\text{--}130 h^{-1}$ Mpc is shown in a sample of galaxies randomly drawn from a population of uniform distribution.

It seems difficult to ascribe the systematic detection of this same scale from many different samples, including the rather sparse one examined here, to chance coincidences. While we were writing this paper, evidence for excess power on the $100 h^{-1}$ Mpc scale was also found in a 2D power spectrum analysis of the Las Campanas Redshift Survey (Landy et al. 1996), further supporting the idea that wavenumbers in the $\sim 100\text{--}200 h^{-1}$ Mpc range have a particular meaning in the structuring of our Universe. One natural possibility is simply that both 1D (skewers) and 2D (slices) projections amplify and enhance a true maximum in the three-dimensional power spectrum. This maximum is expected in all variants of cold dark matter models, as the signature of the horizon size at the epoch of matter–radiation equivalence. Observationally, the spectrum has to turnover around these scales, to be able to connect the very large-scale estimates from microwave anisotropy measurements (e.g. Hu, Sugiyama & Silk 1996), to the $\sim 100 h^{-1}$ Mpc-scale direct measurements from galaxy redshift surveys (e.g. Lin et al. 1996). To produce the observed quasi-regular distribution of objects, the spectrum turnover has to be rather sharp (Frisch et al. 1995). Intuitively, the sharper the 3D peak is, the better a well-defined preferential cell size is defined. The next generation of redshift surveys of galaxies and clusters (see e.g. Guzzo 1996 for a review), will provide a first possibility to study both 1D skewers and 3D power spectra from the same survey volume, thus allowing final clarification of the issues discussed here.

ACKNOWLEDGMENTS

SE thanks A. Gaspani for useful discussions on power spectra. This paper is based upon data collected at the European Southern Observatory, La Silla, Chile.

REFERENCES

- Amendola L., 1994, *ApJ*, 430, L9
 Bahcall N. A., 1991, *ApJ*, 376, 43
 Broadhurst T. J., Ellis R. S., Shanks T., 1988, *MNRAS*, 235, 827
 Broadhurst T. J., Ellis R. S., Koo D. C., Szalay A. S., 1990, *Nat*, 343, 726 (BEKS)
 Broadhurst T. J., Szalay A., Ellis R., Ellman N., Koo D., 1995, in Maddox S. J., Aragon-Salamanca A., eds, *Wide-Field Spectroscopy and Distant Universe*. World Scientific, Singapore, p. 178
 Burbidge G. R., O'Dell S. L., 1972, *ApJ*, 178, 583
 Dekel A., Blumenthal G. R., Primack J. R., Stanhill D., 1992, *MNRAS*, 257, 715
 Duari D., Das Gupta P., Narlikar J. V., 1992, *ApJ*, 384, 35
 Ettori S., Guzzo L., Tarenghi M., 1995, *MNRAS*, 276, 689 (Paper 1)
 Frisch P., Einasto J., Einasto M., Freudling W., Fricke K. J., Gramann M., Saar V., Toomet O., *astro-ph/9503037*
 Gebhardt K., Beers T. C., 1991, *ApJ*, 383, 72
 Giovanelli R., Haynes M. P., 1991, *ARA&A*, 29, 499
 Guzzo L., 1996, in Coles P., Martinez V. J., Pons-Borderia M.-J., eds, *ASP Conf. Ser. Vol. 94, Mapping, Measuring and Modeling the Universe*. Astron. Soc. Pac., San Francisco, p. 157
 Guzzo L., Collins C. A., Nichol R. C., Lumsden S. L., 1992, *ApJ*, 393, L5
 Hu W., Sugiyama N., Silk J., 1996, *Nat*, in press, *astro-ph/9604166*
 Kaiser N., Peacock J. A., 1991, *ApJ*, 379, 482
 Klemola A. R., 1969, *ApJ*, 74, 80
 Koo D. C., Kron R., 1987, in Hewitt A., Burbidge G., Fang L. Z., eds, *Observational Cosmology*. Reidel, Dordrecht, p. 383
 Landy S. D., Shectman S. A., Lin H., Kirshner R. P., Oemler A. A., Tucker D., 1996, *ApJ*, 456, L1
 Lin H., Kirshner R. P., Shectman S. A., Landy S. D., Oemler A., Tucker D. L., Schechter P. L., 1996, *ApJ*, in press, *astro-ph/9606055*
 Mo H. J., Deng Z. G., Xia X. Y., Schiller P., Börner G., 1992, *A&A*, 257, 1
 Shanks T., Stevenson P. R. F., Fong R., MacGillivray H. T., 1984, *MNRAS*, 206, 767
 Strauss M. A., Willick J. A., 1995, *Phys. Rep.*, 261, 271
 Szalay A. S., Ellis R. S., Koo D. C., Broadhurst T. J., 1991, in Holt S. S., Bennett C. L., Trimble V., eds, *After the First Three Minutes*. AIP, New York, p. 261
 Tully R. B., Scaramella R., Vettolani G., Zamorani G., 1992, *ApJ*, 388, 9
 van de Weygaert R., 1991, *MNRAS*, 249, 159
 Vettolani G. et al., 1995, in Maddox S. J., Aragon-Salamanca A., eds, *Wide-Field Spectroscopy and the Distant Universe*. World Scientific, Singapore, p. 115
 Zucca E. et al., 1996, *A&A*, submitted